Eur. J. Mech., B/Fluids, **17**, n° 1, 33-50, 1998

Nonlinear analysis on the natural convection between vertical plates in the presence of a horizontal magnetic field

M. NAGATA *

ABSTRACT. – Finite-amplitude secondary motions of an electrically conducting fluid between two vertical parallel plates heated differntially in the presence of a horizontal magnetic field are obtained numerically in the limit of a small Prandtl number and a small magnetic Prandtl number. We find that, as in the purely hydrodynamic case with the Hartmann number $H = 0$ examined by Nagata and Busse (1983), the bifurcation of the secondary flows is supercritical at the critical Grashof number $G = G_c$ when H is small. Subcritical bifurcations occur at higher wavenumbers. As H is increased, the occurrence of the subcritical bifurcations moves gradually towards a smaller wavenumber region along the neutral curve. For $H = 10$ subcritical motions dominate across the whole range of wavenumbers. The stability analysis shows that the stability of the supercritical motions for small H is bounded by an onset of monotonically growing instability at a higher Grashof number $G = G_{2,c}$. The stability region ($G_c < G < G_{2,c}$) becomes smaller with $G_{2,c}$ approaching G_c from above as H is increased. The region vanishes completely at $H \simeq 7$. © Elsevier, Paris.

1. Introduction

When a viscous fluid is heated from the side, the resultant horizontal temperature gradient induces a shear motion, called natural convection, in the vertical direction. In view of enhancing heat transfer by natural convection, various configurations have been investigated in engineering and industrial applications. For its simple geometry, fluid motion with an inflectional velocity profile between two vertical parallel walls maintained at different temperatures has attracted special attention (*see* for example, Rudakov, 1967; Vest and Arpaci, 1969; Korpela *et al.* 1973; Mizushima and Gotoh, 1975; Gershuni and Zhukhovitskii, 1976; Chen and Pearlstein, 1989; Fujimura, 1992; Takashima, 1994).

The stability characteristic of the basic motion in a vertical slot depends on the Prandtl number, P, defined by the ratio of the thermal diffusivity to the kinematic viscosity of the working fluid. It is widely known that the linear critical mode is stationary for small Prandtl numbers, whereas a Hopf type is prefered for large Prandtl numbers. The sift from the stationary mode (hydrodynamic instability mode) to the Hopf mode (thermal instability mode) occurs at about $P \simeq 12.454$ (Chen and Pearlstein, 1989; Fujimura, 1992).

In order to elucidate hydrodynamic mechanisms for the bifurcation from the basic laminar state to higher levels of transitional state in the natural convection in a slot,

* School of Mathematics and Statistics, The University of Birmingham, Edgbaston, Birmingham, B15 2TT, UK.

EUROPEAN JOURNAL OF MECHANICS, B/FLUIDS, VOL. 17, N° 1, 1998
0997-7546/98/01/© Elsevier, Paris

Nagata and Busse (1983) suppressed thermal instabilities completely by considering the limit of small Prandtl numbers. They found that steady secondary flows with transverse rolls bifurcate supercritically and their stability regions in the wavenumber-Grashof number plane are bounded from the side by the Eckhaus instabilities and from above by an onset of monotonically growing instabilities. The latter has led to the bifurcation of a stable steady tertiary flow which is subharmonic in the streamwise direction with an additional periodicity in the spanwise direction. Small Prandtl numbers are characteristic to liquid metals. Recently, Takashima (1994) investigated the linear stability of a natural convection in a vertical slot in the presence of a transverse magnetic field by assuming a small limit of the magnetic Prandtl number. The present paper extends his analysis to a nonlinear regime.

In geophysical and astrophysical problems where liquid metals with small magnetic Prandtl numbers represent the core of the earth and stars, it is often vital to understand interactions between shear motions and magnetic fields (Proctor and Gilbert, 1994). The limit of small magnetic Prandtl numbers is also typical to liquid metals used in fusion reactor blankets (Girshick and Kruger, 1986; Molokov, 1993; Molokov and Bühler, 1994; Molokov and Stieglitz, 1995 and references therein). Although the Hartmann numbers treated in this paper are not necessarily as high as those for practical use, the knowledge of natural magneto-convection with a moderate magnitude of the Hartmann number should contribute towards the study of the case with a strong field.

The assumption of the small magnetic Prandtl number has also been used by Nagata (1996), where he considers nonlinear three-dimensional solutions in plane Couette flow modified by a transverse magnetic field. We will exploit the method by Nagata (1996), to be referred to as I hereafter, to obtain nonlinear secondary motions in the present analysis. It should be emphasised, however, that the nonlinear interaction mechanisms between the two problems are completely different: three-dimensional distrubances in Nagata (1996) include two-dimensional streamwise vortex components, whereas the present analysis is concerned with two-dimensional spanwise-independent distrubances.

We formulate the problem and derive the basic equations in Section 2. We obtain fully nonlinear secondary solutions numerically in Section 3, followed by a stability analysis on the secondary solutions in Section 4. We discuss the results in Section 5 and conclude the present study in Section 6.

2. Formulation of the problem

We consider an electrically conducting fluid with electric conductivity σ and magnetic permeability μ lying between two parallel vertical plates of infinite extent separated by the distance L in the gravitational field. Constant temperatures, T_1 and T_2, are prescribed on the electrically insulating plates. The horizontal temperature gradient due to the differential heating of the plates causes a variance of the buoyancy force and, as the result, a shear motion in the vertical direction is induced inside the slot. The fluid motion is modified by the Lorentz force when a uniform magnetic field, B_0, permeates horizontally. The kinematic viscosity, ν, and the thermal diffusivity, κ, of the fluid are

assumed to be constant. Further, we assume that the fluid is incompressible with a density ρ expressed by

$$\rho = \rho_0 \{1 - \gamma (T - T_0)\}, \tag{1}$$

where γ is the coefficient of cubical expansion and T_0 is the average temperature $T_0 = \frac{1}{2}(T_1 + T_2)$. With the Boussinesq approximation, the motion is described by the equation of continuity,

$$\nabla \cdot \mathbf{U} = 0, \tag{2}$$

the conservation of momentum,

$$\frac{\partial \mathbf{U}}{\partial t} + (\mathbf{U} \cdot \nabla)\,\mathbf{U} = -\nabla \Pi + (\Theta - \Theta_0)\,\hat{\mathbf{i}} + \nabla^2 \mathbf{U} + \frac{H^2}{P_m}(\nabla \times \mathbf{B}) \times \mathbf{B}, \tag{3}$$

the absence of magnetic monopoles,

$$\nabla \cdot \mathbf{B} = 0, \tag{4}$$

the induction equation,

$$P_m \left\{ \frac{\partial \mathbf{B}}{\partial t} - \nabla \times (\mathbf{U} \times \mathbf{B}) \right\} = \nabla^2 \mathbf{B}, \tag{5}$$

and the temperature equation,

$$P \left\{ \frac{\partial \Theta}{\partial t} + \mathbf{U} \cdot \nabla \Theta \right\} = \nabla^2 \Theta, \tag{6}$$

where

$$H = B_0 L \sqrt{\sigma/\mu}, \tag{7}$$

is the Hartmann number,

$$P_m = \mu \sigma \nu, \tag{8}$$

is the magnetic Prandtl number, and

$$P = \frac{\nu}{\kappa} \tag{9}$$

is the Prandtl number. In the governing equations above, the velocity $\mathbf{U}$, the pressure Π, the magnetic field $\mathbf{B}$ and the temperature Θ (and also Θ_0 from T_0) have been

normalised by ν/L, $\rho_0 \nu^2/L^2$, B_0 and $(T_2 - T_1)/G$ respectively, where G is the Grashof number defined by

$$G = \frac{\gamma g (T_2 - T_1) L^3}{\nu^2}. \tag{10}$$

We have used the scales L^2/ν and L to non-dimensionalise time and all length variables respectively. We take the origin of the Cartesian coordinates at the midchannel with the unit vectors, $\hat{\mathbf{i}}$, $\hat{\mathbf{j}}$ and $\hat{\mathbf{k}}$, in the vertical upward direction, x, the spanwise direction, y, and the direction z, normal to the plates respectively (*Fig.* 1).

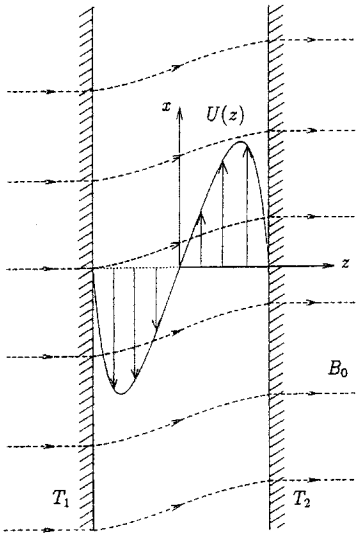

Fig. 1. – Physical configuration.

The no-slip velocity, fixed temperatures and the electrically insulating conditions are prescribed on the plates at $z = \pm\frac{1}{2}$:

$$\mathbf{U} = 0, \tag{11}$$

$$\Theta = \frac{G}{2} \frac{T_1 + T_2 \pm (T_2 - T_1)}{T_2 - T_1} = \Theta_0 \pm \frac{G}{2}, \tag{12}$$

$$\hat{\mathbf{k}} \cdot \nabla \times \mathbf{B} = 0. \tag{13}$$

In addition, the magnetic field of the fluid must be matched to the potential field in the insulating exterior. However, it will be found later that this additional constraint for the magnetic field does not influence the present analysis. (There is no need to specify the boundary condition for the quantity h to be defined in (42). *See* also Nagata, 1996.)

Following I, we assume that the magnetic Prandtl number P_m is small. The limit of small magnetic Prandtl numbers is appropriate for liquid metals used in MHD power

generators. The limit is also characteristic to the liquid core of the earth and magnetic stars. Finite Hartmann numbers are typical of flows in these situations.

We expand $\mathbf{U}$, Π, $\mathbf{B}$, and $\Theta - \Theta_0$ in powers of $P_m \ll 1$, *i.e.*

$$\mathbf{U} = \mathbf{u}^{(0)} + P_m\,\mathbf{u}^{(1)} + P_m^2\,\mathbf{u}^{(2)} + \cdots, \tag{14}$$

$$\Pi = p^{(0)} + P_m\,p^{(1)} + P_m^2\,p^{(2)} + \cdots, \tag{15}$$

$$\mathbf{B} = \mathbf{b}^{(0)} + P_m\,\mathbf{b}^{(1)} + P_m^2\,\mathbf{b}^{(2)} + \cdots, \tag{16}$$

$$\Theta - \Theta_0 = \theta^{(0)} + P_m\,\theta^{(1)} + P_m^2\,\theta^{(2)} + \cdots, \tag{17}$$

and it is easily found that the leading order problem admits

$$\mathbf{b}^{(0)} \equiv \hat{\mathbf{k}}. \tag{18}$$

At the next order the equations,

$$\nabla \cdot \mathbf{u}^{(0)} = 0, \tag{19}$$

$$\frac{\partial \mathbf{u}^{(0)}}{\partial t} + (\mathbf{u}^{(0)} \cdot \nabla)\,\mathbf{u}^{(0)} = -\nabla p^{(0)} + \nabla^2\,\mathbf{u}^{(0)} + H^2\,(\nabla \times \mathbf{b}^{(1)}) \times \hat{\mathbf{k}}, \tag{20}$$

$$\nabla \cdot \mathbf{b}^{(1)} = 0, \tag{21}$$

$$\nabla^2\,\mathbf{b}^{(1)} = -(\hat{\mathbf{k}} \cdot \nabla)\,\mathbf{u}^{(0)}, \tag{22}$$

$$P\left\{\frac{\partial \theta^{(0)}}{\partial t} + \mathbf{u}^{(0)} \cdot \nabla\,\theta^{(0)}\right\} = \nabla^2\,\theta^{(0)}, \tag{23}$$

are obtained in a closed form and must be solved subject to the boundary conditions

$$\mathbf{u}^{(0)} = 0, \tag{24}$$

$$\hat{\mathbf{k}} \cdot \nabla \times \mathbf{b}^{(1)} = 0, \tag{25}$$

$$\theta^{(0)} = \pm\frac{G}{2}, \tag{26}$$

at $z = \pm\frac{1}{2}$. Solutions in higher orders could be obtained successively.

The first order system, (19)-(26), accommodates the basic laminar flow solution

$$\mathbf{u}^{(0)} = U(z)\,\hat{\mathbf{i}}, \qquad \mathbf{b}^{(1)} = B(z)\,\hat{\mathbf{i}}, \qquad \theta^{(0)} = \Theta(z), \tag{27}$$

where

$$U(z) = \frac{G}{H^2}\left(z - \frac{\sinh Hz}{2\sinh H/2}\right), \tag{28}$$

$$B(z) = -\frac{G}{2H^2}\left(z^2 - \frac{1}{4} - \frac{\cosh Hz - \cosh Hz/2}{H\sinh H/2}\right), \tag{29}$$

and

$$\Theta(z) = Gz. \tag{30}$$

It should be noted that the tangential component of the magnetic field is continuous across the insulating boundaries because $B(\pm\frac{1}{2}) = 0$ from (29). In the limit $H \to 0$ we recover the purely hydrodynamic case,

$$U(z) \sim -\frac{G}{6}z\left(z^2 - \frac{1}{4}\right) + O(H^2), \qquad B(z) \sim O(1). \tag{31}$$

We are interested in the situation where the fields are deviated from the basic state by the amount, $\mathbf{u}$, $\mathbf{b}$, p and θ. The deviations satisfy

$$\nabla \cdot \mathbf{u} = 0, \tag{32}$$

$$\begin{aligned}\frac{\partial \mathbf{u}}{\partial t} + +U(z)\frac{\partial \mathbf{u}}{\partial z} + (\hat{\mathbf{k}}\cdot\mathbf{u})\,U'(z)\,\hat{\mathbf{i}} + (\mathbf{u}\cdot\nabla)\,\mathbf{u} \\ = -\nabla p + \theta\,\hat{\mathbf{i}} + \nabla^2\,\mathbf{u} + H^2\,(\nabla\times\mathbf{b})\times\hat{\mathbf{k}},\end{aligned} \tag{33}$$

$$\nabla \cdot \mathbf{b} = 0, \tag{34}$$

$$\nabla^2\,\mathbf{b} = -(\hat{\mathbf{k}}\cdot\nabla)\,\mathbf{u}, \tag{35}$$

$$P\left\{\frac{\partial\theta}{\partial t} + U(z)\frac{\partial\theta}{\partial z} + G(\hat{\mathbf{k}}\cdot\mathbf{u}) + \mathbf{u}\cdot\nabla\theta\right\} = \nabla^2\,\theta\,, \tag{36}$$

where the prime denotes the ordinary differentiation with respect to z. The boundary conditions are

$$\mathbf{u} = 0, \tag{37}$$

$$\hat{\mathbf{k}} \cdot \nabla \times \mathbf{b} = 0, \tag{38}$$

and

$$\theta = 0 \tag{39}$$

at $z = \pm\frac{1}{2}$.

In the limit of small Prandtl numbers we obtain

$$\theta \equiv 0 \tag{40}$$

from (36) and (39), so that the thermal perturbations can be ignored completely for the rest of the analysis.

For convenience, we separate $\mathbf{u}$ and $\mathbf{b}$ into the average parts $\bar{\mathbf{u}} \equiv \breve{U}(t, z)\,\hat{\mathbf{i}}$ and $\bar{\mathbf{b}} \equiv \breve{B}(t, z)\,\hat{\mathbf{i}}$, and residuals $\breve{\mathbf{u}}$ and $\breve{\mathbf{b}}$, respectively, where the average denoted by an overbar is taken in the x and y directions. The residuals are solenoidal and they are further separated into two parts as follows:

$$\mathbf{u} = \bar{\mathbf{u}} + \breve{\mathbf{u}} = \breve{U}(t, z)\,\hat{\mathbf{i}} + \nabla \times \nabla \times \hat{\mathbf{k}}\,\phi + \nabla \times \hat{\mathbf{k}}\,\psi, \tag{41}$$

$$\mathbf{b} = \bar{\mathbf{b}} + \breve{\mathbf{b}} = \breve{B}(t, z)\,\hat{\mathbf{i}} + \nabla \times \nabla \times \hat{\mathbf{k}}\,h + \nabla \times \hat{\mathbf{k}}\,g. \tag{42}$$

The xy-averages of ϕ, ψ, h, and g are zero by definition. The total mean fields, $\hat{U}(t, z)$ and $\hat{B}(t, z)$, now include $\breve{U}(t, z)$ and $\breve{B}(t, z)$:

$$\hat{U}(t, z) = U(z) + \breve{U}(t, z), \qquad \hat{B}(t, z) = B(z) + \breve{B}(t, z). \tag{43}$$

Applying the operations $\hat{\mathbf{k}} \cdot \nabla\times$ and $\hat{\mathbf{k}}\cdot$ to equation (35) yields

$$\nabla^2 \Delta_2 h = -\partial_z \Delta_2 \phi, \tag{44}$$

$$\nabla^2 \Delta_2 g = -\partial_z \Delta_2 \psi, \tag{45}$$

where ∂ is the partial differential operator with respect to its subscript and $\Delta_2 = \partial^2_{xx} + \partial^2_{yy}$ is the two-dimensional Laplacian operator. The relationship between $\breve{U}$ and $\breve{B}$ is obtained by taking the xy-average of the x component of (35):

$$\partial^2_{zz} \breve{B} = -\partial_z \breve{U}. \tag{46}$$

By taking into account of the fact that $\breve{U}$ is antisymmetric in z, we obtain

$$\breve{B}(t, z) = -\int_{-\frac{1}{2}}^{z} \breve{U}(t, z)\,dz, \tag{47}$$

where we have used $\breve{U}(\pm\frac{1}{2}) = \breve{B}(\pm\frac{1}{2}) = 0$.

Applying the $\hat{\mathbf{k}} \cdot \nabla \times \nabla \times$ and $\hat{\mathbf{k}} \cdot \nabla \times$ to Eq. (33) yields

$$(48)\quad (\hat{U}\,\partial_x - \nabla^2 + \partial_t)\,\nabla^2\,\Delta_2\,\phi - (\partial_z^2\,\hat{U})\,\partial_x\,\Delta_2\,\phi + H^2\,\partial_z^2\,\Delta_2\,\phi + \hat{\mathbf{k}}\cdot\nabla\times\nabla\times[\breve{\mathbf{u}}\cdot\nabla\,\breve{\mathbf{u}}] = 0,$$

$$(49)\quad (\hat{U}\,\partial_x - \nabla^2 + \partial_t)\,\Delta_2\,\psi - (\partial_z\,\hat{U})\,\partial_y\,\Delta_2\,\phi + H^2\,\partial_z^2\,\nabla^{-2}\,\Delta_2\,\psi - \hat{\mathbf{k}}\cdot\nabla\times[\breve{\mathbf{u}}\cdot\nabla\,\breve{\mathbf{u}}] = 0,$$

where h and g have been eliminated by substituting for ϕ and ψ using (44) and (45). The inverse Laplacian operator ∇^{-2} in (49) is expressed in I. The equations for $\breve{U}$ are obtained by taking the xy-average of the x component of (33):

$$(50)\quad -\partial_t\,\breve{U} + \partial_z^2\,\breve{U} - H^2\,\breve{U} + \partial_z\,\overline{\Delta_2\,\phi\,(\partial_x^2\,\phi + \partial_y\,\psi)} = 0,$$

where (46) is used to eliminate $\breve{B}$. The boundary conditions at $z = \pm\frac{1}{2}$ now become

$$(51)\quad \phi = \partial_z\,\phi = \psi = \breve{U} = 0.$$

There is no need to specify the boundary conditions for h and g.

Comparison of (48), (49) and (50) with the basic equations for the purely hydrodynamic case by Nagata and Busse (1983) (*see* their Eqs. (2.7a), (2.7b) and (2.8)) reveals that the effects of the magnetic field, namely those additional terms with the coefficients H^2 in (48)-(50), do not change the symmetry.

3. Nonlinear secondary motions

It is known from the linear theory that as the Hartmann number increases the critical Grashof number increases while the corresponding critical wavenumber decreases (Takashima, 1994; Fujimura and Nagata, 1997). Since the imaginary part of the linear eigenvalue at the onset of the two-dimensional instability is zero the secondary flows with transverse rolls must be steady. Therefore, we expand ϕ and $\breve{U}$ in the following way:

$$(52)\quad \phi\,(x,\,z) = \sum_{\ell=1}^{\infty}\,\sum_{m=-\infty}^{\infty}\,a_{\ell,\,m}\,e^{im\,\alpha\,x}\,f_\ell\,(z),$$

$$(53)\quad \breve{U}\,(z) = \sum_{k=1}^{\infty} c_k\,\sin\,2\,k\,\pi\,z,$$

where the functions, $f_\ell\,(z)$,known as the Chandrasekhar functions, satisfy $f_\ell\,(\pm\frac{1}{2}) = f_\ell'\,(\pm\frac{1}{2}) = 0$ (Chandrasekhar, 1961).

Since ϕ is real, we require

$$(54)\quad a_{\ell,\,-m}^{*} = a_{\ell,\,m}$$

where the asterisk denotes the complex conjugate. Due to the symmetry of the problem, the nonlinear interactions are restricted to the case with

$$a^*_{\ell,m} = \begin{cases} a_{\ell,m} & (\ell : \text{odd}) \\ -a_{\ell,m} & (\ell : \text{even}) \end{cases} \tag{55}$$

The set (55) is identical to the one used by Nagata and Busse (1983).

For numerical purposes the infinites series in (52) and (53) must be truncated so that only those components with $a_{\ell,m}$, and c_k, whose subscripts satisfy

$$\ell + |m| < N_T, \qquad k < N'_T, \tag{56}$$

are taken into account. The resulting finite set of nonlinearly interacting components is determined in terms of their amplitudes, $a_{\ell,m}$, and c_k numerically by using the Galerkin method combined with the Newton-Raphson method. Table I checks the convergence of the nonlinear calculations for various truncation levels in terms of the deviation of the momentum transport

$$\breve{M}_t = -\frac{d}{dz}\breve{U}, \tag{57}$$

from the basic laminar state. In the following calculations the truncation level $(N_T, N'_T) = (14, 12)$ is employed for $H = 2$, and $(16, 14)$ for $H = 6$ and 10.

TABLE I. – The momentum transport at various truncation levels.

N_T, N'_T	$H = 2$ $\alpha = 2.65,\ G = 10,000$	$H = 6$ $\alpha = 2.2,\ G = 35,000$
10,8	10.3734	
11,9	10.3187	
12,10	10.2795	13.7347
13,11	10.2565	12.9617
14,12	10.2337	12.2334
15,13	10.2300	12.0999
16,14	10.2237	11.9023
17,15	10.2225	11.8639
18,16		11.7855

4. Stability analysis of the secondary motions

In order to analyse the stability of the secondary solutions, we superimpose the general form of three-dimensional perturbations,

$$\tilde{\phi}(x, y, z; t) = \sum_{\ell=1}^{\infty} \sum_{m=-\infty}^{\infty} \tilde{a}_{\ell,m}\, e^{im\alpha x} f_\ell(z)\, e^{idx+iby+\sigma t} \tag{58}$$

$$\tilde{\psi}(x, y, z; t) = \sum_{\ell=1}^{\infty} \sum_{m=-\infty}^{\infty} \tilde{b}_{\ell, m} e^{im\alpha x} \sin l\pi \left(z + \frac{1}{2}\right) e^{idx+iby+\sigma t}. \tag{59}$$

It will be found that the following two equations, linear with respect to $\tilde{\phi}$ and $\tilde{\psi}$,

$$\begin{aligned}(\hat{U}\partial_x - \nabla^2 + \partial_t)\nabla^2\Delta_2\tilde{\phi} - \hat{U}''\partial_x\Delta_2\tilde{\phi} + H^2\partial_{zz}^2\Delta_2\tilde{\phi} \\ + \hat{\mathbf{k}}\cdot\nabla\times\nabla\times[\breve{\mathbf{u}}\cdot\nabla\tilde{\mathbf{u}} + \tilde{\mathbf{u}}\cdot\nabla\breve{\mathbf{u}}] = 0,\end{aligned} \tag{60}$$

$$\begin{aligned}(\hat{U}\partial_x - \nabla^2 + \partial_t)\Delta_2\tilde{\psi} - \hat{U}'\partial_y\Delta_2\tilde{\phi} + H^2\partial_{zz}^2\nabla^{-2}\Delta_2\tilde{\psi} \\ - \hat{\mathbf{k}}\cdot\nabla\times[\breve{\mathbf{u}}\cdot\nabla\tilde{\mathbf{u}} + \tilde{\mathbf{u}}\cdot\nabla\breve{\mathbf{u}}] = 0,\end{aligned} \tag{61}$$

where

$$\tilde{\mathbf{u}} = \nabla\times\nabla\times\hat{\mathbf{k}}\tilde{\phi} + \nabla\times\hat{\mathbf{k}}\tilde{\psi}, \tag{62}$$

are sufficient to describe the stability of the secondary motions. In contrast to the expression for ϕ in (52), the summations (58) and (59) include $m = 0$. The contributions from $m = 0$ in the summations correspond to the perturbation for the mean flow. As $d^2 + b^2$ tends to zero for $m = 0$, (60) could represent the mean flow perturbation equation corresponding to (50). Perturbations $\tilde{\phi}$ and $\tilde{\psi}$ satisfy the boundary conditions at $z = \pm\frac{1}{2}$

$$\tilde{\phi} = \partial_z\tilde{\phi} = \tilde{\psi} = 0. \tag{63}$$

Regarding the stability Eqs. (60) and (61), it can be verified that among all the components in the summations (58) and (59), the following two sets,

$$\text{(I)}: \begin{cases} \tilde{a}_{\ell,-m} = \begin{cases} \tilde{a}_{\ell,m} & (\ell : \text{even}) \\ -\tilde{a}_{\ell,m} & (\ell : \text{odd}) \end{cases} \\ \tilde{b}_{\ell,-m} = \begin{cases} \tilde{b}_{\ell,m} & (\ell : \text{even}) \\ -\tilde{b}_{\ell,m} & (\ell : \text{odd}) \end{cases} \end{cases} \tag{64}$$

$$\text{(II)}: \begin{cases} \tilde{a}_{\ell,-m} = \begin{cases} \tilde{a}_{\ell,m} & (\ell : \text{odd}) \\ -\tilde{a}_{\ell,m} & (\ell : \text{even}) \end{cases} \\ \tilde{b}_{\ell,-m} = \begin{cases} \tilde{b}_{\ell,m} & (\ell : \text{odd}) \\ -\tilde{b}_{\ell,m} & (\ell : \text{even}) \end{cases} \end{cases} \tag{65}$$

are independent for $d = 0$, $b \neq 0$, while the following two sets,

$$(\mathrm{III}) : \tilde{b}_{\ell,m} \equiv 0, \tag{66}$$

and

$$(\mathrm{IV}) : \tilde{a}_{\ell,m} \equiv 0, \tag{67}$$

are also independent for $d \neq 0$, $b = 0$. When $db \neq 0$, (64) unites with (65) and (66) with (67). The resulting two unions are equal.

After truncating the system with the same truncation criteria as was used for obtaining the finite amplitude solutions,

$$\ell + |m| < N_T, \tag{68}$$

we take the Galerkin projection of the Eqs. (60) and (61) to derive the eigenvalue problem

$$\mathbf{A}\mathrm{x} = \sigma\,\mathbf{B}\mathbf{x}, \tag{69}$$

with the growth rate, σ, as the eigenvalue. The elements of the vector $\mathbf{x}$ are composed of perturbation amplitudes $\tilde{a}_{\ell m}$ and $\tilde{b}_{\ell m}$. The real matrices $\mathbf{A}$ and $\mathbf{B}$ are functions of the finite amplitude solution at given G, H, and α as well as the Floquet parameter pair (d, b). We solve (69) numerically using the QZ algorithm implemented in NAG routine F02BJF.

The truncation level dependency of σ for typical parameter values is shown in Table II. To be consistent with the truncation levels used in obtaining the nonlinear solutions, we choose $N_T = 14$ and $N_T = 16$ for the stability analyses at $H = 2$ and $H \geq 6$, respectively.

TABLE II. – The growth rate σ at various truncation levels. $b = 1.6$.

N_T, N'_T	$H = 2$ $\alpha = 2.65$ $G = 10,000$ $d = 0$	$H = 2$ $\alpha = 2.65$ $G = 10,000$ $d = 1.325$	$H = 6$ $\alpha = 2.2$ $G = 35,000$ $d = 0$	$H = 6$ $\alpha = 2.2$ $G = 35,000$ $d = 1.1$
10,8	(– 1.8101, ± i 14.8116)	(2.0934,0)		
11,9	(– 1.8374, ± i 14.8056)	(2.0790,0)		
12,10	(– 1.8587, ± i 14.7925)	(2.0634,0)	(0.7995, ± i 18.8794)	(11.3701,0)
13,11	(– 1.8666, ± i 14.7840)	(2.0552,0)	(0.3470, ± i 18.6693)	(10.8485,0)
14,12	(– 1.8772, ± i 14.7747)	(2.0456,0)	(– 0.1244, ± i 18.4600)	(10.3123,0)
15,13	(– 1.8785, ± i 14.7737)	(2.0445,0)	(– 0.2103, ± i 18.4245)	(10.2146,0)
16,14	(– 1.8815, ± i 14.7711)	(2.0418,0)	(– 0.3440, ± i 18.3669)	(10.0613,0)
17,15	(– 1.8819, ± i 14.7707)	(2.0414,0)	(– 0.3684, ± i 18.3557)	(10.0326,0)
18,16			(– 0.4217, ± i 18.3325)	(9.9709,0)

It is easily seen from the sets (64), (65), (66) and (67) that the growth rate σ is periodic in d with the period α provided the infinite number of modes are taken into account. Since $\mathbf{A}(d, b)$ and $\mathbf{B}(d, b)$ are real, and $\mathbf{A}(-d, -b)$ and $\mathbf{B}(-d, -b)$ correspond to complex conjugate perturbations, σ is symmetric in d and b. (This is a consequence from

the antisymmetric nature of the mean velocity profile in z.) From these arguments, it suffices to evaluate σ only in $0 \leq d \leq \frac{1}{2}\alpha$ and $b \geq 0$.

5. Results

5.1. $H = 2$

All the nonlinear solutions obtained for $H = 2\,(\alpha < 3.5)$ bifurcate supercritically. The wavenumber which gives the maximum momentum transport is shifted towards larger values.

Figure 2 plots the growth rate on $d/\alpha = 0.0,\ 0.1,\ 0.2,\ 0.3,\ 0.4$ and 0.5 at $H = 2$ and $G = 10,000\,(> G_c)$ with three different wavenumbers $\alpha = 2.3,\ 2.65$ and 3.0. It is seen that for $\alpha = 2.65$, which corresponds to the critical wavenumber for $H = 2$ in the linear stability analysis, the transverse roll solutions is already unstable to monotonically growing three-dimensional perturbations at $G = 10,000$. (*Fig.* $2b$). Figures $2a$ and $2c$ show that for the wavenumber away from the central region the growth of three dimensional perturbations is suppressed, whereas the Eckhaus instability on $b = 0$ becomes dominant. Figure 3 pinpoints the onset of various instability modes in the $\alpha - G$ plane for $H = 2$.

The figure shows that the stability of the transverse roll solutions above the neutral curve is bounded from the side by the Eckhaus instability limit and from above by the onset of monotonically growing three-dimensional instabilities. Since $d = \frac{1}{2}\alpha$ on the latter boundary, three-dimensional tertiary flows, subharmonic in the streamwise direction, should bifurcate. Also shown in the figure is the onset of an oscillatory instability at higher G, which occurs with $d = 0$ and $b \neq 0$. This mode could be recognised by the dashed curves for $d/\alpha = 0$ in Figure 2, though $\mathrm{Re}\,[\sigma] < 0$

5.2. $H = 6$

The stability region in the $\alpha - G$ plane reduces its size in the case of $H = 6$ as can be seen from Figure 4. The reduction of the stability region with increasing H is quite apparent by the comparison of the stability diagram for the hydrodynamic case with $H = 0$ by Nagata and Busse (1983), $(G/G_c < 1.004$ for $H = 6$ and $G/G_c < 1.04$ for $H = 0)$. The transverse vortex structure of the secondary flow and the induced magnetic field at $\alpha = 2.2$, $G = 34,700$ inside the stability region are exhibited in Figure 5. Since the Grashof number $G = 34,700$ is just above the critical value $(G/G_c \simeq 1.003)$, the mean flow $U\,(z)$ and the mean field $B\,(z)$ are modified only slightly.

As will be discussed in the next subsection, the most profound effect of the magnetic field is the existence of subcritical secondary motions for higher Hartmann numbers. The existence of the solution below the neutral curve begins to show up at larger wavenumbers for $H = 6$ in Figure 4.

5.3. $H = 10$

Further calculations indicated that at $H = 7$ the bifurcation of the secondary flow with the critical wavenumber becomes subcritical. The stability analysis shows that both the lower and the upper branches of the secondary flow with the critical wavenumber

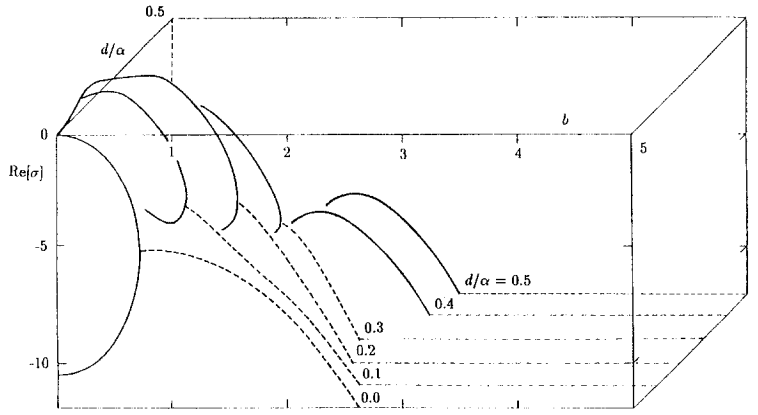

(a)

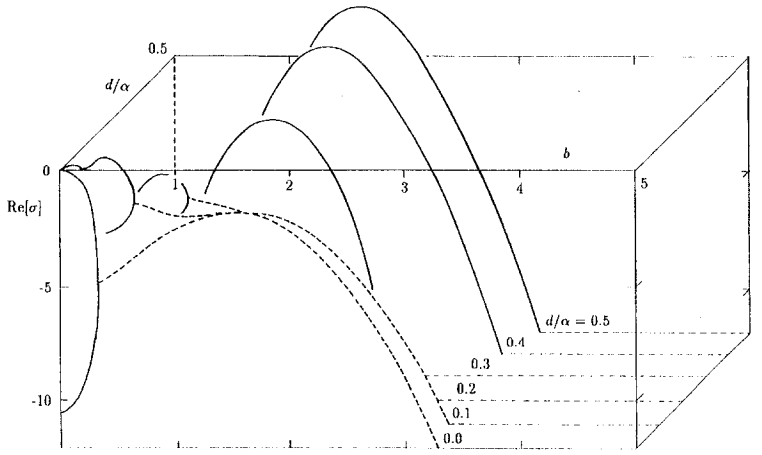

(b)

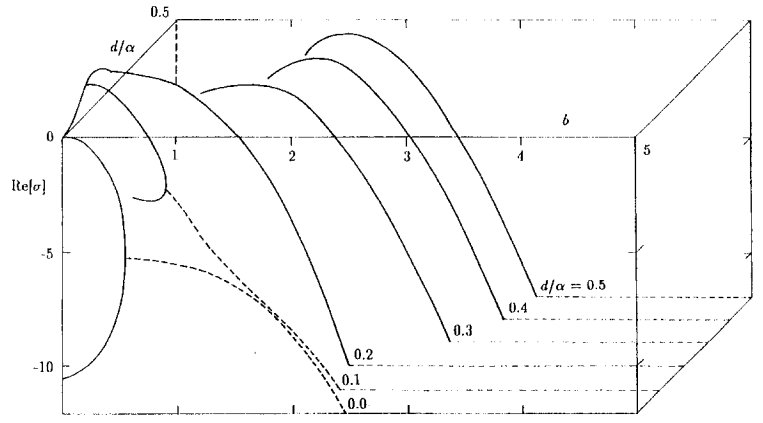

(c)

Fig. 2. – The growth rate, σ, on $(d,\ b)$ for $G = 10,000$ and $H = 2$.
(a) $\alpha = 2.3$, (b) $\alpha = 2.65$, (c) $\alpha = 3.0$. σ is real/complex on solid/broken lines.

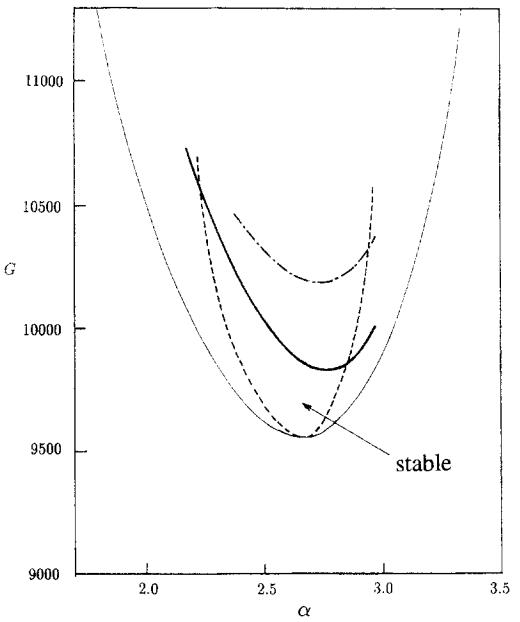

Fig. 3. – The stability diagram on the $\alpha - G$ plane for $H = 2$. The stability of the transverse roll solution above the neutral curve (thin solid line) is bounded by the Eckhaus stability limit (broken line) and the monotonically growing three-dimensional instability (thick solid line). The oscillatory instability sets in on the dash-dotted line.

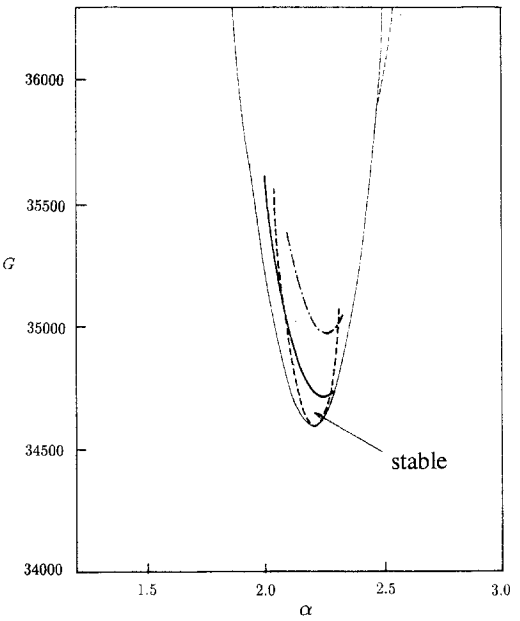

Fig. 4. – The stability diagram on the $\alpha - G$ plane for $H = 6$. The stability of the transverse roll solution is bounded by the Eckhaus stability limit (broken line) and the monotonically growing three-dimensional instability (thick solid line). The oscillatory instability sets in on the dash-dotted line. The neutral curve is given by thin solid line. The solutions bifurcate subcritically for $\alpha > 2.45$. The minimum Grashof numbers, *i.e.* limit points, on the subcritical branch at large wavenumbers are given by the thin broken line.

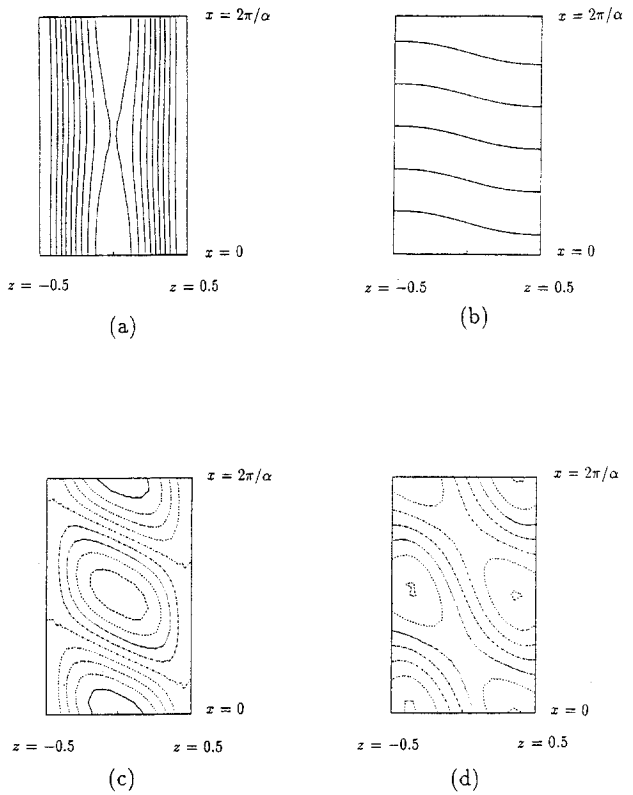

Fig. 5. – The stable secondary state at $\alpha = 2.2$, $G = 34,700$ and $H = 6$. (a) The stream function of the total flow. (b) The lines of the total magnetic force calculated with $P_m = 0.01$. (c) The stream function deviated from the basic laminar state. (d) The lines of the magnetic forces deviations.

are unstable: perturbations which have the same spatial structure as the secondary flow, namely those with $d = b = 0$, are responsible for the instability of the lower branch, while three-dimensional perturbations with $d = \frac{1}{2}\alpha$ and $b \neq 0$, are responsible for the upper branch. It is unlikely that there exist stable secondary motions at all for $H > 7$. Therefore, we present only the nonlinear solutions for $H = 10$.

The three curves for $G = 300,000$, $200,000$ and $150,000$, at $H = 10$ in Figure 6 do not intersect with $\breve{M}_t = 0$, indicating the existence of subcritical solutions even at almost half the critical Grashof number. The curve for $G = 300,000$ is not closed. Instead, one end of the branch terminates at the point A in the figure where all the modes with even $m\,(= 2\,m')$ vanish. Since $\alpha\, m = 2\,\alpha \times m'$, the solution at A corresponds to the solution at A' on the same branch, *i.e.* the branch terminates on itself. The other end B also terminates on itself with the wavenumber tripled: Only the modes with m being an integer multiple of three are non-zero at the point B. The wavenumber at B' in the figure is not exactly three times as the wavenumber at B. The discrepancy is due to the fact that almost two-thirds of the total modes are zero, resulting in the actual reduction of the truncation level. The termination of the solution branch on itself was reported by Nagata and Busse (1983) in the hydrodynamic case $(H = 0)$. The incapability of obtaining nonlinear solutions for small wavenumber in their analysis was resolved by Fujimura (1992) where

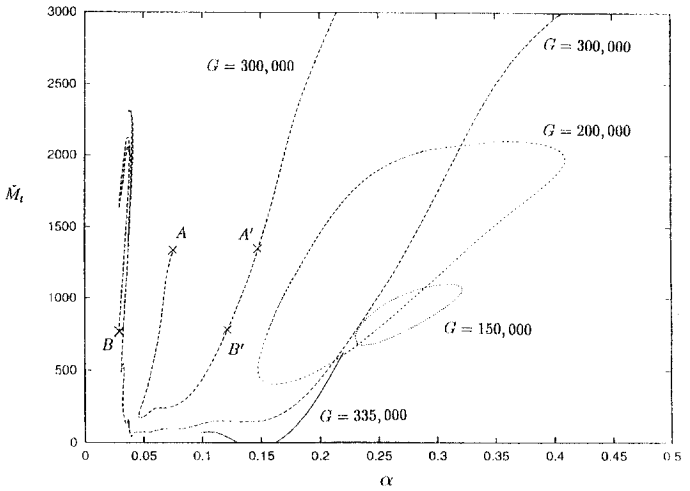

Fig. 6. – The momentum transport, $\check{M}_t$, of the nonlinear solutions for $H = 10$.

he considered resonant interaction of neutral modes whose wavenumber ratio is 1:2. The interaction takes place *above* the neutral curve for the hydrodynamic case, whereas here the interaction in the magnetohydrodynamic case occurs in the subcritical region. The complex behaviour of the nonlinear solutions with much richer structures due to the resonant interaction of the modes whose wavenumber ratio is 1:2 near the degenerate bifurcation point (*i.e.* near the point on the neutral curve where the bifurcation changes from supercritical to subcritical) in the magnetohydrodynamic case will be discussed separately (Fujimura and Nagata, 1997).

In addition to the main nonlinear solution branch, several isolated branches are also detected in the smaller wavenumber region for $H = 10$; in order to avoid confusion, these are not shown in the figure. Branches isolated from the main branch in the smaller wavenumber region outside the neutral curve of the Bénard convection have also been discussed by Nagata (1995).

6. Conclusion

The steady two-dimensional secondary motions in natural convection in the presence of an applied transverse magnetic field are presented and their stability is investigated for $0 < H \leq 10$. In the analysis, the limit of a small Prandtl number and a small magnetic Prandtl number is considered in view of possible applications to liquid metal flows. The secondary flow bifurcates supercritically for small H, provided that wavenumbers are not very large. Since the critical Grashof number increases as the Hartmann number increases, the magnetic field has a stabilising effect on the natural convection.

Stability analysis of the nonlinear secondary flows reveals that as H is increased from zero the second critical Grashof number, $G = G_{2,c}$, where monotonically growing three-dimensional instabilities set in, approaches the linear (first) critical Grashof number G_c, reducing the stability region of the secondary motion from above in the $\alpha - G$

plane. As H in increased, the transition from supercritical bifurcations which occurs at a large wavenumber, moves along the neutral curve towards a smaller wavenumber region gradually. As the bifurcation at the critical wavenumber becomes subcritical at $H \simeq 7$, the stability region of the secondary flow vanishes completely. No stable secondary flows are expected to exists for $H > 7$. The whole wavenumber region is dominated by subcritical solutions at $H = 10$.

Therefore, the question arises: what kind of flows are physically realised when the applied magnetic field is strong? Three-dimensional tertiary motions, which should bifurcate at $G = G_{2,c}$, may be stable and physically realised for higher Hartmann numbers. Also, new types of motion due to resonant interactions in the subcritical region may be possible. Degenerate mode interactions with wavenumber ratio 1:2, where one mode changes its bifurcation nature from supercritical on the neutral curve, have been reported by Fujimura and Nagata (1997).

Acknowledgements

The author thanks the Japan Atomic Energy Research Institute for its kind invitation as a Visiting Fellow in the summer/autumn of 1994 while he was on a study leave. A part of the present research was carried out during that period.

REFERENCES

CHANDRASEKHAR S., 1961, *Hydrodynamic and Hydromagnetic Stability*, Dover New York.

CHEN Y.-M., PEARLSTEIN A. J., 1989, Stability of free-convection flow of variable-viscosity fluids in vertical and inclined slots, *J. Fluid Mech.*, **198**, 513-541.

FUJIMURA K., 1992, Higher harmonic resonances in free convection between vertical parallel plates, *Phil. Trans. R. Soc. Lond. A*, **340**, 95-130.

FUJIMURA K., MIZUSHIMA J., 1991, Nonlinear equilibrium solutions for traveling waves in a free convection between vertical parallel plates, *Eur. J. Mech. B/Fluids*, **10**, n° 2-Suppl., 25-30.

FUJIMURA K., NAGATA M., 1997, Degenerate 1:2 steady mode interactions – MHD flow in a vertical slot, *Physica D*, (submitted).

GERSHUNI G. Z., ZHUKHOVITSKII E. M., 1976, *Convective Stability of Incompressible Fluids*, Keter, Jerusalem.

GIRSHICK S. L., KRUGER C. H., 1986, Experimental study of secondary flows in a magnetohydrodynamic channel, *J. Fluids Mech.*, **170**, 233-252.

KORPELA S. A., GÖZÜM D., BAXI C. B., 1973, On the stability of the conduction regime of natural convection in a vertical slot, *Int. J. Heat Mass Transfer*, **16**, 1683-1690.

MIZUSHIMA J., GOTOH K., 1975, The stability of natural convection in a vertical fluid layer, *J. Fluid Mech.*, **73**, 65-75.

MOLOKOV S., 1993, Fully developed liquid-metal flow in multiple rectangular ducts in a strong uniform magnetic field, *Eur. J. Mech., B/Fluids*, **12**, n° 6, 769-787.

MOLOKOV S., BÜHLER L., 1994, Liquid metal flow in a U-bend in a strong uniform magnetic field, *J. Fluid Mech.*, **267**, 325-352.

MOLOKOV S., STIEGLITZ R., 1995, Liquid-metal flow in a system of electrically coupled U-bends in a strong uniform magnetic field, *J. Fluid Mech.*, **299**, 73-95.

NAGATA M., BUSSE F. H., 1983, Three-dimensional tertiary motions in a plane shear layer, *J. Fluid Mech.*, **135**, 1-26.

NAGATA M., 1995, Bifurcations at the Eckhause points in two-dimensional Rayleigh-Bénard convection, *Phys. Rev. E.*, **52** (6), 6141-6145.

NAGATA M., 1996, Nonlinear solutions of modified plane Couette flow in the presence of a transverse magnetic field, *J. Fluid Mech.*, **307**, 231-243.

PROCTOR M. R. E., GILBERT A. D., 1994, *Lectures on Solar and Planetary Dynamos*, Cambridge University Press.

RUDAKOV R. N., 1967, Spectrum of perturbations and stability of convective motion between vertical planes, *Prikl. Mat. Mekh.*, **31**, 349-355, Translated in *J. Appl. Math. Mech.*, **31**, 376-383.

TAKASHIMA M., 1994, The stability of natural convection in a vertical layer of electrically conducting fluid in the presence of a transverse magnetic field, *Fluid Dyn. Res.*, **14**, 121-134.

VEST C. M., ARPACI V. S., 1969, Stability of natural convection in a vertical slot, *J. Fluid Mech.*, **36**, 1-15.

(Manuscript received February 12, 1997;
revised May 28, 1997;
accepted June 18, 1997.)